Hydrobiologia (2010) 655:149–158
DOI 10.1007/s10750-010-0417-2

PRIMARY RESEARCH PAPER

Diel depth distributions of microbenthos in tidal creek sediments: high resolution mapping in fluorescently labeled embedded cores

Matthew R. First · James T. Hollibaugh

Received: 4 January 2010 / Revised: 26 June 2010 / Accepted: 16 August 2010 / Published online: 3 September 2010

Abstract Intertidal sediments experience substantial changes in temperature, salinity, and solar irradiation over short time periods. We applied the Fluorescently Labeled Embedded Core (FLEC) technique to map distribution patterns of microbenthos in tidal creek sediments. Our aims were to determine if micro-scale distributions varied over the course of a day and to test the null hypothesis that microbenthos are randomly distributed. Eight samples were collected at 3 h intervals from an intertidal sandflat on Sapelo Island, Georgia, USA. Cores were incubated with CellTracker Green (CMFDA, hereafter, CTG), a fluorogenic compounds that accumulates in metabolically active cells. Cores were embedded with epoxy and examined with laser scanning confocal microscopy. Image analysis was used to map the vertical locations of active microbenthos, which in these sediments consisted of benthic microalgae (BMA), ciliates, and flagellates. Microbenthos were abundant over the entire depth profiled (2 cm), although O_2 microelectrode profiles indicate that only the top 3 mm of sediment was oxygenated during high light (1,000 μE m^{-2} s^{-1}). More than 91% of organisms mapped were <22 μm in diameter and, based upon size and cell appearance, were BMA. Microbenthos accumulated in the top 1 mm at 0800 and 1100 h, corresponding to both low tide and high solar irradiation. This pattern conforms to BMA migratory rhythms determined by other methods. The standardized Morisita's Index of dispersion determined that CTG-positive objects were significantly clumped at all time points and at each of the three spatial scales examined. This clumping pattern likely results from the heterogeneous distribution of resources, such as prey items for phagotrophs and dissolved nutrients or growth substrates for autotrophs or heterotrophs.

Keywords Tidal creeks · Sapelo Island · Salt marsh · Microzoobenthos · Microphytobenthos · Migrations · Ciliates · Meiofauna · Embedded cores

Handling editor: Stuart Jenkins

M. R. First · J. T. Hollibaugh
Department of Marine Sciences, The University of Georgia, Athens, GA 30602-3636, USA

M. R. First (✉)
Department of Geology and Geophysics, Woods Hole Oceanographic Institution, 211 Watson, MS#52, Woods Hole, MA 02543, USA
e-mail: mfirst@whoi.edu

Introduction

Intertidal sediments are dynamic environments, subject to rapid changes in tidal cover, temperature, salinity, and irradiation. Many microbenthic organisms (defined here as protists and metazoan meiofauna) are motile and can adjust to these changing physical and chemical gradients over the day. For

example, both benthic diatoms (Consalvey et al., 2004) and ciliates (Saburova et al., 2004) undergo vertical migrations. The spatial distribution patterns of microbenthos sets the frequency of interactions (e.g., predator–prey encounter rate) and can reveal resource gradients.

Shallow-water sediments support high rates of primary production by benthic microalgae (BMA) that, in turn, are important to the sustenance and growth of both epibenthic and pelagic invertebrates (MacIntyre et al., 1996; Miller et al., 1996). Variable primary production throughout the day results in a shifting depth of dissolved oxygen availability, restructuring the fine-scale distributions of benthic protists (Fenchel & Jansson, 1966; Böttcher et al., 2000; Gücker & Fischer, 2003). Macrofaunal bioturbations (e.g., burrowing behavior) interspersed along the surface of the sediment results in locations with higher rates of solute flux—forming horizontal resource gradients (Goni-Urriza et al., 1999). The physical and biological factors leading to spatial heterogeneity influence the survival and activity of benthic microorganisms and, therefore, are critical to overall benthic metabolism.

Several techniques have been used to measure the vertical distributions of microbenthos in marine sediments. BMA have received the most attention and a variety of approaches are used to detect their location and movement in the sediments (reviewed by Consalvey et al., 2004). Commonly, sediment cores are extruded and subsampled periodically with depth. BMA concentration and diversity of organisms can be analyzed by extracting chlorophyll *a* (Pinckney & Zingmark, 1993) or DNA (Reed et al., 2006). Sectioning sediment cores can yield highly resolved depth distributions of benthic microorganisms (e.g., MacIntyre & Cullen, 1995). Yet, the horizontal distribution and fine-scale spatial relationships among microbenthos cannot be determined when vertical sections are homogenized.

The Fluorescently Labeled Embedded Core (FLEC) technique was developed to detect the life positions of protists and meiofauna in sediment with high spatial resolution (Bernhard et al., 2003). Organisms in sediment cores are labeled with a fluorogenic compound. The core is then chemically preserved, dehydrated, and subsequently embedded in epoxy. Locations of organisms in the sediment matrix are stable and can be mapped. We used the FLEC technique to examine the micro-scale changes in the distribution and associations of microbenthos (here, eukaryotes <200 μm, typically BMA, ciliates, and flagellates) in a tidal creek sandflat over a diel cycle. The goal of this study was to observe the distribution of microbenthos over the course of a day and to determine if the spatial distribution varied more with distance (between replicate cores) or time points. Spatial distributions influence the rates of interactions among organisms (e.g., competition for resources, predation pressure, and genetic exchange) and are crucial to overall ecosystem function (Nunan et al., 2007).

Methods

Sampling

We sampled an area of sandflat in the bed of a tidal creek (Dean Creek) on Sapelo Island, a 67 km^2 barrier island on the Georgia coast, during 28–29 July, 2005. Dean Creek is a tidal channel bisecting *Spartina alterniflora* salt marsh at the southern end of the island. The sampling location was a 2 m^2 area of intertidal non-vegetated sandflat adjacent to and immediately downstream of the Dean Creek Nature Trail bridge (31.3946°N, 81.2700°W), roughly 2 km from the mouth of the creek. The plot was flat and level with no crab burrows and the sediment surface was uniform in color. Sediment was collected at 3 h intervals starting at 0600 h using an Ekman grab sampler (15 cm^2) lowered from the bridge. Resampling the same area was avoided by marking the location where the grabs were taken on the bridge deck. Care was taken to deploy and retrieve the grab smoothly and slowly so that the sediment in the grab was minimally disturbed during the sampling. Cores were approximately 8–10 cm in depth. The sediment surface was not visibly disturbed and no cracks were observed in the grab. The sediment adjacent to the grab sampler walls (which was likely disrupted during the sampling) was not used in this experiment.

Upon retrieval, the unopened sampler was carefully placed in a bucket filled with creek water (except during low tide when sediments were exposed) and transported to the lab at the University of Georgia Marine Institute within 10 min. As soon as the Ekman grab was opened, small sub-cores were

collected for FLEC analysis. The properties of the sediment (grain size, porosity, organic matter content) and evaluation of the microbenthic community (including chlorophyll *a* concentrations, and protist and bacterial counts) were performed and are reported elsewhere (First & Hollibaugh, 2008). A Seabird conductivity, temperature, and depth sensor (CTD, SBE-19) was placed in the creek about 1 m away from the sandflat with its sensors at roughly the same depth as the sample plot. Water temperature, salinity, depth, and Photosynthetically Active Radiation (PAR) were recorded every 60 s during the course of the sampling series. PAR was recorded with a 4π sensor, and detects light reflected from the sandy sediment surface. Thus, these measurements do not represent the absolute incident PAR on the surface. Rather, these measurement indicate the timing and relative intensity of incident PAR.

Fluorescently labeled embedded cores

The FLEC technique was originally designed and applied to deep sea microbial mats in fine sediments (Pike et al., 2001; Bernhard et al., 2003). A thorough description of the FLEC technique is available elsewhere (Bernhard et al., 2003). Four sub-cores roughly 3 cm long were collected from each grab sample using 10 ml plastic syringes with the tips removed and beveled to reduce compaction upon coring. These cores were collected roughly 10 cm apart, then treated and analyzed separately. The 10 cm distance between cores is between 3 and 4 orders of magnitude greater than the size of organisms being investigated. Thus, we treat these cores as independent replicates that capture the small-scale variability within the sandflat examined (Heffner et al., 1996). Cotton was added to the syringe to support the sediment; rubber stoppers with holes capped the syringe and allowed for fluid movement. Filtered (0.22 µm) seawater (FSW, 0.5 ml) was added to the surface of samples taken when the site was flooded; no FSW was added when sediments were exposed at low tide. Microbenthos were labeled by adding of 25 µl of 1 mM of CellTracker Green chloromethylfluorescein diacetate (Invitrogen, hereafter, CTG) solution to the top of the core. Syringes were placed upright in 100 ml containers filled with FSW to roughly 75% of the sediment height (allowing for movement of the CTG through the top 2 cm of sediment) and incubated for 2 h. Note that sample identifiers are based on the time that incubations were stopped, rather than when the core was collected. Cores collected during daylight hours were exposed to indirect sunlight through south-facing windows during the incubation and samples collected at night were covered to exclude artificial light. CTG concentrations and the incubation duration were determined in preliminary experiments to be adequate for the CTG to permeate into the sediment, be taken up and transformed under the conditions encountered during this study. Cores were then fixed with 8% electron microscopy grade glutaraldehyde and kept upright in the dark at 4 ± 2°C until further processing.

Fixed cores were progressively dehydrated with FSW: ethanol (10, 30, 50, 80%, and three rinses of 100% ethanol) by allowing a volume roughly 3× the sediment volume to pass through the core. Anhydrous cupric sulfate was used to dehydrate the 100% ethanol used for the final rinses. Care was taken to always keep sediments submerged. Equal weights of a two-part, low viscosity epoxy resin (Embed-It™, Polysciences) were mixed with 100% dehydrated ethanol and used for one rinse. Finally, two rinses of 100% epoxy (each equal to the volume of the sediment) were passed through the sediment core. Flow was stopped before all of the second rinse had passed though sediments, then the epoxy was polymerized at 50°C for 72 h. The solidified cores were stored at room temperature away from light. At least three of the four sub-cores from each grab sample survived the embedding process and polymerized.

Embedded cores were cut along the long axis with a thin-blade diamond saw. Both halves of the split core were polished with progressively finer grit (up to 600 grit) to produce a flat, uniform surface. The polished surface was examined at 100× magnification using a Leica Laser Scanning Confocal Microscope (LSCM) with excitation at 488 nm by an argon/krypton laser (dichroic mirror: 500 nm, range: 510–525 nm, pinhole: 1.6× airy). The high sand content of the sediment cores restricted laser light penetration to ~20 µm into the exposed face. Infrared multiphoton illumination did not allow for deeper penetration into the core, so we did not adopt this alternative method. The location of the maximum pixel value encountered in 14 to 16 images taken along the axis of penetration was used to determine the position of active cells. Image editing software (Adobe Photoshop) was used to adjust the brightness and contrast of images to equalize minor

differences in display range. The three dimensional images were flattened along the axis of laser light penetration to yield a two-dimensional map, each image representing 1.5 mm^2 of the sediment. This third axis contained much less spatial information ($\sim$20 μm) and flattening did not cause significant overlapping or obscuring of objects. The map images were then assembled to form a 1.5 × 20 mm profile along the depth of the core. The top of the sediment core was often uneven; therefore, we defined the position of the 10th fluorescent object encountered along a vertical scan from the highest point of the sediment surface as zero depth and discarded the objects above this depth. One vertical profile was assembled for each core. The dimensions, area and vertical position of fluorescent objects >12 μm^2 ($\sim$3.8 μm equivalent circular diameter—ECD), were measured with image analysis software (ImagePro Plus 4.1). This size threshold excludes individual bacterial cells and small bacterial aggregates. This size range included larger organisms, such as nematodes. Thus, the term "microbenthos" as used here includes nematodes, even though they are generally referred to as meiofauna.

In salt marsh sediments, BMA represent a large portion of the microbial biomass. However, CTG-positive cells could not be categorized as BMA based upon chlorophyll *a* fluorescence as the dehydration series necessary for embedding cores in epoxy also extracts photopigments. Many of the organisms could be identified as pennate diatoms by their morphology; other eukaryotes such as ciliates can also be roughly identified by shape. However, there is a potential for misidentifying objects, especially for organisms longer or wider than 20 μm, as cell orientation relative to the plane of observation can disguise true shape. Therefore, we only used the two-dimensional size to categorize objects. Nematodes could be identified by size, even when they were sectioned along a transverse plane (See Fig. 3D).

Oxygen profiles

A second set of sediment cores (1.5 cm diameter syringe, $\sim$3 cm depth) was collected from the site at low tide on 30 July, 2005. These cores were stored at 24 ± 3°C under a natural light regime and transported to Athens, GA for analysis. Oxygen concentration profiles in the cores were determined 2 days later. A microelectrode with a 50 μm tip (Revsbech & Jørgensen, 1983) was lowered through the sediment at 100 μm intervals after the sediment was equilibrated in high light ($\sim$1,000 μE m^{-2} s^{-1}) or darkness for at least 10 min. The electrode was calibrated at O_2 saturation and at anoxia by measuring the stable voltage reached after bubbling FSW with air, or at $\sim$3 cm sediment depth in a core, respectively. Estimates of O_2 concentration (μM) were calculated as linear interpolations between the voltage at zero O_2 and at calculated O_2 saturation at the salinity and temperature of FSW.

Analysis

Microbenthos distributions were analyzed by two methods. First, the two-dimensional dispersion of microbenthos was evaluated via Morisita's standardized index of dispersion (I_M) (Krebs, 1989). This index indicates whether microbenthos are randomly, uniformly, or unevenly (clumped or patchily) dispersed. When $1 > I_M > 0.5$, microbenthos are significantly under-dispersed (clumped) according to a χ^2 distribution (alpha = 0.025, df = number of quadrats − 1). Likewise, when $-1 < I_M < -0.5$, microbenthos are significantly over-dispersed (uniform); and when $0.5 > I_M > -0.5$ microbenthos are randomly dispersed (Krebs, 1989). Each profile was trimmed by 0.25 mm on each side to account for the slight lateral drift of the microscope as images were collected along the long axis of the core, yielding a 1 × 20 mm profile. Morisita's index was calculated for each profile using quadrat sizes of 0.25 × 0.25 mm, 0.5 × 0.5 mm, and 1.0 × 1.0 mm, yielding 320, 80, or 20 quadrats for the entire profile, respectively. A computer algorithm to sort objects to quadrants and to perform calculations and statistical analyses was written in MatLab 6.1. The average I_M was calculated from the three profiles at each time point for each quadrat size.

Second, the relative inequality of the depth distribution was calculated by the Gini Coefficient of Inequality (G), which is a non-parametric measure of distribution unevenness (Dixon et al., 1987; Dixon 1988):

$$G = \frac{1}{\overline{X}\, n\,(n-1)} \sum_{i=1}^{n} (2i - n - 1) X_i$$

where X is the number of objects in depth bin i (sorted from the most populated to least populated

bin), and n is the sample size. The Gini Coefficient is 0 for a perfectly even distribution and approaches perfect inequality at 1. The degree of unevenness in depth distribution was based upon the mean percent difference between the observed number of microbenthos in each depth interval and the expected number in each interval assuming an even distribution with depth. Unlike Morisita's index of dispersion, the Gini coefficient only measures the distribution along one dimension (depth); therefore, there was no need to trim the profiles as was done for the two-dimensional analysis described above. All data from each time point were pooled and objects were binned into 50 equal depth intervals. Bootstrapping analysis (2000 replicates) was used to calculate the 95% confidence intervals (CI) of the bias-corrected Gini Coefficient (Stats Direct 2.5). The mean depth was calculated from the positions of all microbenthos observed in each of the three replicate profiles.

Results

Salinity at the study site fluctuated between 19 and 24 and temperature ranged from 29.0 to 34.6°C over the study period (Fig. 1A); the water depth over the sampling site ranged from 0 to 1.2 m (Fig. 1B). Sediments were exposed once during daylight hours (0925–1204 h) and again during the night (2340–0026 h). The top 1 cm of sediment had a density of 1.46 g cm^{-3}, mean grain size of 0.26 mm (±0.11 SD), porosity of 0.41 (±0.12 SD), and an organic matter content of 2.0% (±0.4 SD). Microelectrode profiles revealed supersaturating O_2 concentrations at about 1 mm depth during high illumination (Fig. 2). However, no O_2 was detected below 3 mm depth at high light and without light, O_2 at 1 mm was <7% of saturation and was not detectable below 2 mm.

The FLEC technique yielded high contrast images of CTG-positive cells in all cores examined (Fig. 3). At all time points, the majority of microbenthos (>90% of total) mapped in FLEC depth profiles were smaller than 22 µm ECD (Fig. 4). This size range of organisms is mostly composed of small diatoms, flagellates, and small ciliates (First & Hollibaugh, 2008).

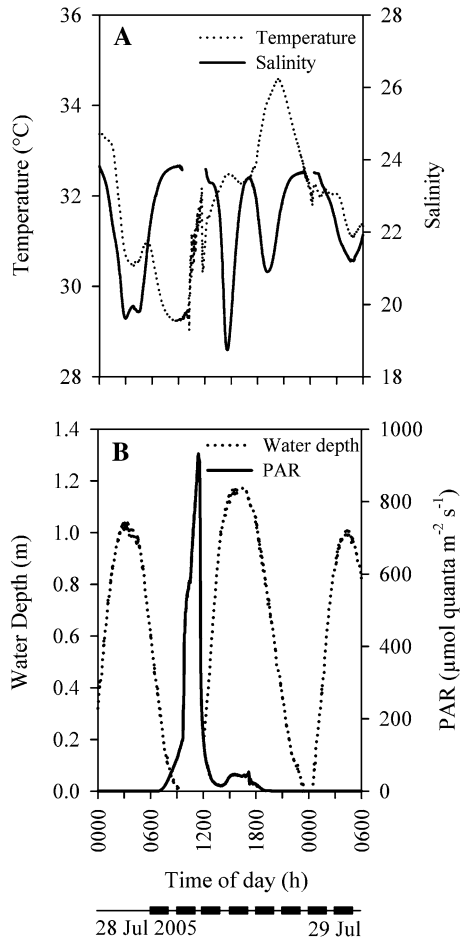

Fig. 1 **A** Temperature, salinity, **B** water depth and photosynthetically active radiation (PAR) in Dean Creek, Sapelo Island, Georgia between 28 and 29 Jul 2005. *Timeline bars* show CTG incubation durations

Although there was no measurable O_2 at depths >3 mm, active cells were found over the entire 20 mm profile. Microbenthos were non-randomly and unevenly dispersed at all time points in all replicate cores at all spatial scales examined. The mean Morisita index (I_M) was >0.5 at all time points, indicating that microbenthos were significantly clumped. Also, I_M was >0.5 for all quadrat sizes examined and increased with increasing quadrat size (Fig. 5).

Data from the three cores for each sample were pooled for analysis of depth distributions of microbenthos (average n = 2,301, range: 772–5,043). Microbenthos were most abundant near the surface at 0800 and 1100 h, corresponding to a pattern of

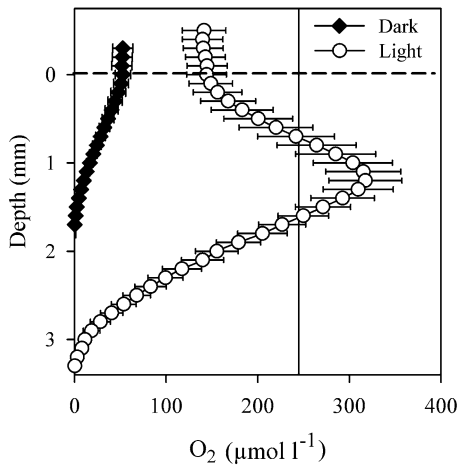

Fig. 2 Oxygen concentration profiles in light and dark-adapted Dean Creek sediment cores. The *vertical line* indicates the dissolved O_2 saturation at in situ salinity and temperature. Mean (*line and points*) and standard error (*bars*) are based on a total of 8 profiles from 2 cores

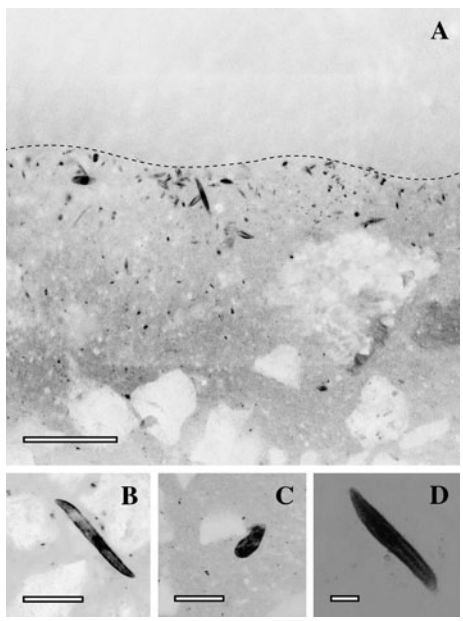

Fig. 3 Example images of microbenthos in FLEC cores collected from the 1500 h FLEC core. **A** Microbenthos clustered at the sediment surface, denoted by a *dotted line*, scale bar = 300 µm. Examples of microbenthos: **B** a pennate diatom, **C** a ciliate, and **D** a portion of a nematode. Scale bars = 100 µm. Images were *inverted* for clarity (i.e., dark objects were fluorescent)

migration to the sediment surface during tidal emersion and light. A high subsurface concentration between 12 and 14 mm depth was also present at 1100 h.

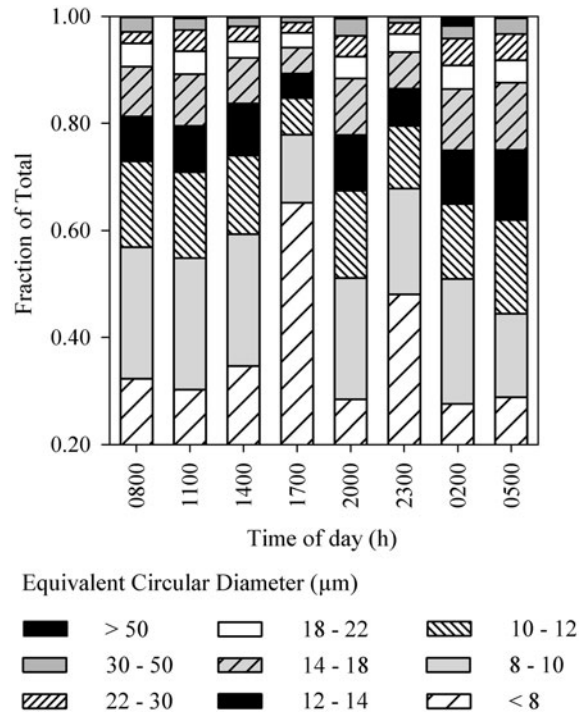

Fig. 4 Size distribution (Equivalent Circular Diameter, ECD) of CTG-positive microbenthos in pooled FLEC core profiles

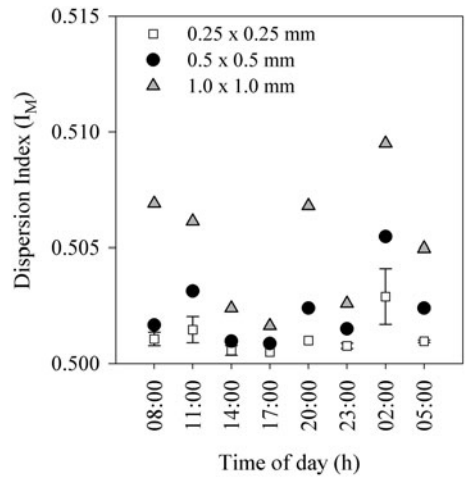

Fig. 5 Dispersion of microbenthos in sediment cores calculated by Morisita's Index (I_M). The spatial scale is defined by the quadrat size (0.25 × 0.25, 0.5 × 0.5 or 1.0 × 1.0 mm). Points show the mean I_M value ($n = 3$, except for 0800 h, where $n = 2$); *SD bars* are only shown for 0.25 × 0.25 mm, *error bars* for other quadrat sizes are omitted for clarity; percent coefficients of variations were <0.1% in these cases. I_M ranges from −1 to 1; the *y*-axis is scaled to show small differences between the quadrat sample sizes

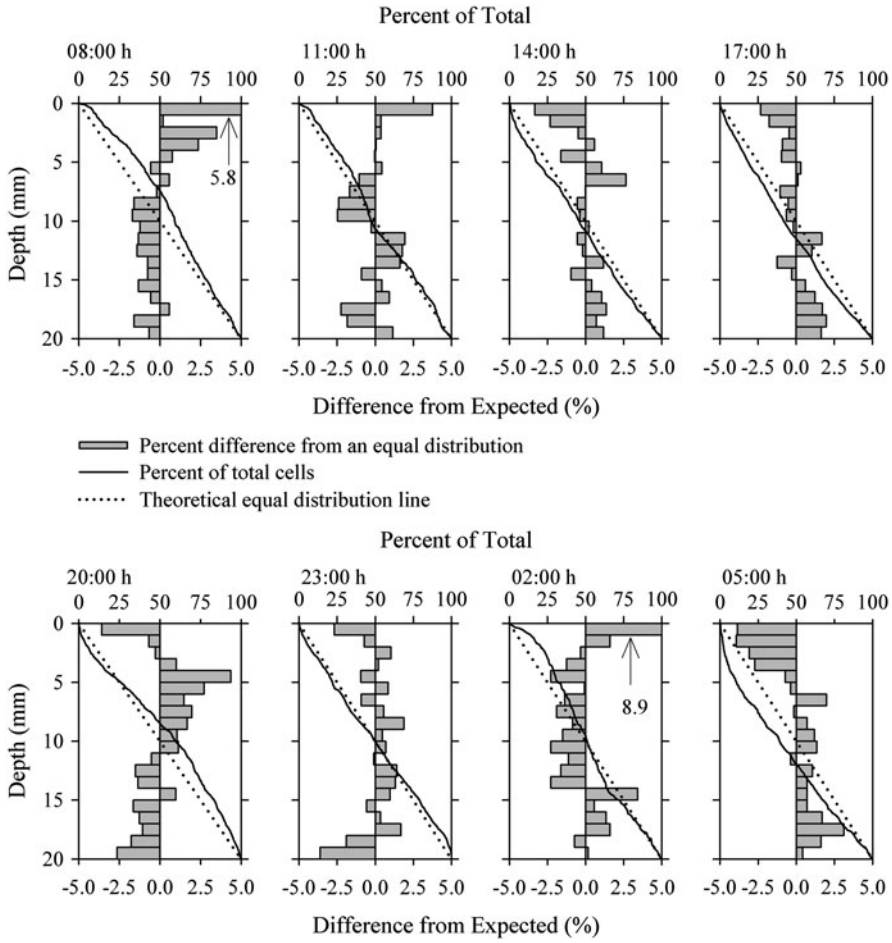

Fig. 6 Vertical distribution of CTG-positive microbenthos in profiles at all time points. *Bars* indicate the percent deviation from the abundance expected in the depth interval if cells were evenly distributed along the profile. Deviations greater than 5% from expected are indicated with *arrows* (at 0800 and 0200 h). *Line plots* indicate the accumulated abundance of microbenthos with depth compared with an even distribution (*dotted line*)

Microbenthos were depleted from the top 3 mm during the afternoon and into the evening and subsurface accumulations were observed in these samples. For instance, microbenthos accumulated between 4 and 11 mm depth at 2000 h (Fig. 6). At 0200 h, microbenthos were most abundant at the sediment surface. At 0500 h microbenthos were depleted from the top 6 mm of sediment.

The relative unevenness (Gini coefficient) ranged from 0.15 (±0.01 CI) to 0.31 (±0.03 CI) throughout the sampling period, with organisms most equally distributed at 1700 and 2300 h (Fig. 7). Usually, as the mean depth of the microbenthos increases, organisms become more equally distributed. The higher Gini coefficient with lower mean depth indicates that microbenthos are unevenly concentrated near the sediment surface. However, the 0500 h profiles do not follow this trend as microbenthos are unevenly distributed with accumulations in deeper sediment horizons.

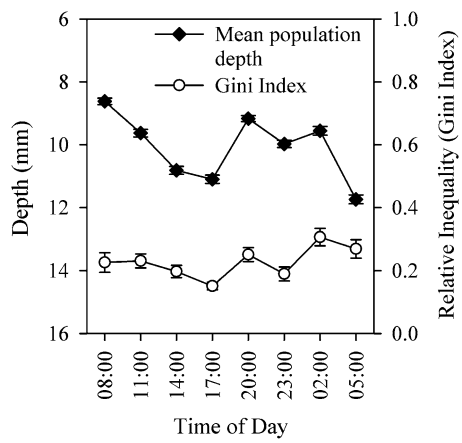

Fig. 7 Mean microbenthos depth and Gini coefficient of inequality of FLEC profiles at all sample times. *Bars* show standard error of mean depth and the 95% confidence interval of the Gini coefficient

Discussion

Despite the shallow depth of oxygen penetration, active microbenthos were found throughout the entire depth examined at all time points. Because the fluorescent stain used in this study only detects enzymatically active microbenthos, the accumulation in deeper sediment horizons cannot be explained as the burial of dead or inactive cells. The presence of CTG-positive cells throughout the depth examined also indicates that CTG was able to permeate completely through at least the upper 20 mm of the core and react within the incubation time.

Overall, microbenthos showed a clumped distribution in all sample profiles. In sandy salt marsh sediments, the aggregation of microbenthos in interstitial spaces might contribute to the clumped dispersion patterns. However, the quadrat sizes used in this analysis were equal to or larger than the mean grain size. The index of dispersion increased with increasing quadrat size (see Fig. 5), indicating that microbenthos were more unevenly dispersed at larger spatial scales. If the dispersion patterns were solely defined by interstitial spaces, then the dispersion would become more uniform with larger quadrats. Instead, the observed distribution of microbenthos is likely driven by aggregation near favorable microhabitats. Sediments are heterogeneous environments with sharp resource gradients; the uneven distribution of the microbenthic community is likely a response to these resource gradients. Symbiotic associations between organisms also result in a clumping of microbial communities. For example, benthic eukaryotes aggregate near sulfide-oxidizing bacteria, perhaps as a refuge from high sulfide concentrations (Bernhard et al., 2003). Also, microbial mats and consortia can lead to highly localized zones of sediment microbial biomass (Boetius et al., 2000; Stal, 2001).

The presence of high densities of BMA in subsurface sediments as we found here is counterintuitive, yet commonly observed (see Pinckney & Zingmark, 1993, and references therein). Light scattering in sandy sediments results in the situation where the highest light intensities are found below the sediment surface (Kühl et al., 1994). A subsurface light intensity maximum, therefore, may explain subsurface accumulations of BMA. Yet high light attenuation results in low light intensity below the top $\sim$2 mm of sediment; BMA found below this depth are unable to obtain light for photosynthesis and are described functionally as "photosynthetically inactive biomass" (Kelly et al., 2001). Diel vertical migrations of BMA are commonly observed in intertidal sediments. The migratory rhythms may function to deter resuspension by tidal flow or predation by surface grazers (MacIntyre et al., 1996). BMA might also migrate into the sediments to access inorganic nutrients (Kingston, 2002). Regardless, subsurface BMA can account for a large portion of total chlorophyll. Inactive, subsurface BMA can contribute the relative constancy of total sediment chlorophyll amid large variations in photosynthetically active surface BMA (Kelly et al., 2001).

The abundance of BMA and other microorganisms found at depth in sediments suggests that most microbenthos can tolerate anoxic and sulfidic sediments. However, O_2 concentrations measured in cores in the lab may not reflect the availability of O_2 to subsurface aerobic microbes in the field. For example, tidal forcing may increase the depth of O_2 penetration (Rusch et al., 2001) and the O_2 concentrations determined in sediment cores may be lower than available in the field during tidal flow. Likewise, bioturbation by microbenthos can extend the depth of O_2 penetration (Glud & Fenchel, 1999; Pike et al., 2001) and allow aerobic respiration. Alternatively, the abundance of aerobic organisms in anoxic sediments may demonstrate spatial heterogeneity of chemical gradients in sediments that is not captured by microelectrode profiling (Bernhard et al., 2003). For example, the movement of meiofauna through anoxic sediments can allow for the highly localized transport of solutes (Pike et al., 2001).

The mean depth of microbenthos varied throughout the day. In general, when the depth was greater than 10 mm (half of the core depth), the vertical distribution became more even. Restated, microbenthos were generally unevenly distributed towards the upper half of the core at most time points. One exception to this was at 0500 h, when microbenthos were unevenly distributed towards the bottom half of the core. This sampling time occurred several hours into flood tide. Therefore, tidal advection may have resuspended microbenthos into the water column, causing a depletion of microbenthos from the surface sediments. The timing and magnitude of microbenthos advection into the water column can be critically important for water column filter feeders, which consume BMA as a significant portion of their diet (Thoresen, 2004).

The spatial distribution of organisms is a fundamental parameter of many ecological processes. The relative distance between individuals reveals competitive and synergistic associations, and reveals how resources are partitioned. Thus, analysis of the microscale distributions of microbenthos can provide insight into the physiology and ecology of sediment eukaryotic microbial communities, and how these communities respond to rapidly shifting environmental conditions. In marine sediments, patchy microbenthos distributions are observed on both vertical (e.g., Saburova et al., 2004) and horizontal spatial scales. For example, BMA horizontal patch size ranges from 10^1 to 10^2 cm^2 (e.g., Blanchard, 1990; Sandulli & Pinckney, 1999). Variations in microbenthos biomass can be overlooked when using sampling techniques with low spatial resolution (Jesus et al., 2005). Using the FLEC technique to map the distribution of microbenthos allows for the detection of subtle variations in spatial distributions of sediment microbial communities.

Acknowledgments This study was supported by NSF Georgia Coastal Ecosystems LTER grant (OCE-9982133). J. Bernhard critically reviewed an earlier draft of this manuscript. S. Joye was generous with the use of her microelectrode probes and provided guidance for this study. We are grateful for the hospitality and logistical support of J. Garbisch and M. Price at the University of Georgia Marine Institute (UGAMI). J. Bernhard, M. Farmer, S. Joye and C. Meile provided guidance on the design of this project. D. Di Iorio and P. McKay (Dept. Marine Sci., UGA) assisted with the CTD. C. Fleisher (Geology Dept., UGA) advised and assisted on the diamond saw operation. C. Keith and J. Shields (Center for Ultrastructural Research, UGA) assisted with confocal microscope operation. M.R.F. was supported by a UGA Graduate School Assistantship. This is contribution no. 957 from UGAMI.

References

Bernhard, J. M., P. T. Visscher & S. S. Bowser, 2003. Submillimeter life positions of bacteria, protists, and metazoans in laminated sediments of the Santa Barbara Basin. Limnology and Oceanography 48: 813–828.

Blanchard, G. F., 1990. Overlapping microscale dispersion patters of meiofauna and microphytobenthos. Marine Ecology Progress Series 68: 101–111.

Boetius, A., K. Ravenschlag, C. J. Schubert, D. Rickert, F. Widdel, A. Gieseke, R. Amann, B. B. Jørgensen, U. Witte & O. Pfannkuche, 2000. A marine microbial consortium apparently mediating anaerobic oxidation of methane. Nature 407: 623–626.

Böttcher, M. E., B. Hespenheide, E. Llobet-Brossa, C. Beardsley, O. Larsen, A. Schramm, G. Wieland, G. Böttcher, U. G. Berninger & R. Amann, 2000. The biogeochemistry, stable isotope geochemistry, and microbial community structure of a temperate intertidal mudflat: an integrated study. Continental Shelf Research 20: 1749–1769.

Consalvey, M., D. M. Paterson & G. J. C. Underwood, 2004. The ups and downs of life in a benthic biofilm: migration of benthic diatoms. Diatom Research 19: 181–202.

Dixon, P., 1988. Correction. Ecology 69: 1307.

Dixon, P. M., J. Weiner, T. Mitchellolds & R. Woodley, 1987. Bootstrapping the Gini coefficient of inequality. Ecology 68: 1548–1551.

Fenchel, T. & B. O. Jansson, 1966. On the vertical distribution of the microfauna in the sediments of a brackish-water beach. Ophelia 3: 161–177.

First, M. R. & J. T. Hollibaugh, 2008. Protistan bacterivory and benthic microbial biomass in an intertidal creek mudflat. Marine Ecology Progress Series 361: 59–68.

Glud, R. N. & T. Fenchel, 1999. The importance of ciliates for interstitial solute transport in benthic communities. Marine Ecology Progress Series 186: 87–93.

Goni-Urriza, M., X. de Montaudouin, R. Guyoneaud, G. Bachelet & R. de Wit, 1999. Effect of macrofaunal bioturbation on bacterial distribution in marine sandy sediments, with special reference to sulphur-oxidising bacteria. Journal of Sea Research 41: 269–279.

Gücker, B. & H. Fischer, 2003. Flagellate and ciliate distribution in sediments of a lowland river: relationships with environmental gradients and bacteria. Aquatic Microbial Ecology 31: 67–76.

Heffner, R. A., M. J. Butler & C. K. Reilly, 1996. Pseudoreplication revisited. Ecology 77: 2558–2562.

Jesus, B., V. Brotas, M. Marani & D. M. Paterson, 2005. Spatial dynamics of microphytobenthos determined by PAM fluorescence. Estuarine, Coastal and Shelf Science 65: 30–42.

Kelly, J. A., C. Honeywill & D. M. Paterson, 2001. Microscale analysis of chlorophyll-*a* in cohesive, intertidal sediments: the implications of microphytobenthos distribution. Journal of Marine Biological Association of the United Kingdom 81: 151–162.

Kingston, M. B., 2002. Effect of subsurface nutrient supplies on the vertical migration of *Euglena proxima* (Euglenophyta). Journal of Phycology 38: 872–880.

Krebs, C. J., 1989. Ecological Methodology. Harper & Row, New York.

Kühl, M., C. Lassen & B. B. Jorgensen, 1994. Light penetration and light intensity in sandy marine sediments measured with irradiance and scalar irradiance fiber-optic microprobes. Marine Ecology Progress Series 105: 139–148.

MacIntyre, H. L. & J. J. Cullen, 1995. Fine-scale vertical resolution of photosynthetic parameters in a shallow-water benthos. Marine Ecology Progress Series 122: 227–237.

MacIntyre, H. L., R. J. Geider & D. C. Miller, 1996. Microphytobenthos: the ecological role of the "secret garden" of unvegetated, shallow-water marine habitats. 1. Distribution, abundance and primary production. Estuaries 19: 186–201.

Miller, D. C., R. J. Geider & H. L. MacIntyre, 1996. Microphytobenthos: the ecological role of the "secret garden"

of unvegetated, shallow-water marine habitats. 2. Role in sediment stability and shallow-water food webs. Estuaries 19: 202–212.

Nunan, N., I. Young, J. Crawford & K. Ritz, 2007. Bacterial interactions at the microscale – linking habitat to function in soil. In Franklin, R. B. & A. L. Mills (eds), The Spatial Distribution of Microbes in the Environment. Springer, Netherlands, Dordrecht: 61–85.

Pike, J., J. M. Bernhard, S. G. Moreton & I. B. Butler, 2001. Microbioirrigation of marine sediments in dysoxic environments: implications for early sediment fabric formation and diagenetic processes. Geology 29: 923–926.

Pinckney, J. & R. G. Zingmark, 1993. Biomass and production of benthic microalgal communities in estuarine habitats. Estuaries 16: 887–897.

Reed, A. J., R. A. Lutz & C. Vetriani, 2006. Vertical distribution and diversity of bacteria and archaea in sulfide and methane-rich cold seep sediments located at the base of the Florida escarpment. Extremophiles 10: 199–211.

Revsbech, N. P. & B. B. Jørgensen, 1983. Photosynthesis of benthic microflora measured with high spatial resolution by the oxygen microprofile method: capabilities and limitations of the method. Limnology and Oceanography 28: 749–756.

Rusch, A., S. Forster & M. Huettel, 2001. Bacteria, diatoms and detritus in an intertidal sandflat subject to advective transport across the water–sediment interface. Biogeochemistry 55: 1–27.

Saburova, M. A., A. I. Azovskii & I. G. Polikarpov, 2004. A comparative analysis of the vertical migrations of interstitial ciliates in different types of sediments. Oceanology 44: 535–547.

Sandulli, R. & J. L. Pinckney, 1999. Patch sizes and spatial patterns of meiobenthic copepods and benthic microalgae in sandy sediments: a microscale approach. Journal of Sea Research 41: 179–187.

Stal, L. J., 2001. Coastal microbial mats: the physiology of a small-scale ecosystem. South African Journal of Botany 67: 399–410.

Thoresen, M., 2004. Temporal and Spatial Variation in Seston Available to Oysters and the Contribution of Benthic Diatoms to Their Diet in the Duplin River, Georgia. University of Georgia, Athens.